Haematopoietic stem cell differentiation promotes the release of prominin-1/CD133-containing membrane vesicles—a role of the endocytic–exocytic pathway

*Nicola Bauer[1], Michaela Wilsch-Bräuninger[2†], Jana Karbanová[1†], Ana-Violeta Fonseca[1†], Doreen Strauss[1], Daniel Freund[1], Christoph Thiele[2], Wieland B. Huttner[2], Martin Bornhäuser[3,4], Denis Corbeil[1,3]**

Keywords: CD133; cell differentiation; exosome; haematopoietic stem cell; lipid raft

DOI 10.1002/emmm.201100147

Received October 18, 2010
Revised March 25, 2011
Accepted April 11, 2011

The differentiation of stem cells is a fundamental process in cell biology and understanding its mechanism might open a new avenue for therapeutic strategies. Using an *ex vivo* co-culture system consisting of human primary haematopoietic stem and progenitor cells growing on multipotent mesenchymal stromal cells as a feeder cell layer, we describe here the exosome-mediated release of small membrane vesicles containing the stem and cancer stem cell marker prominin-1 (CD133) during haematopoietic cell differentiation. Surprisingly, this contrasts with the budding mechanism underlying the release of this cholesterol-binding protein from plasma membrane protrusions of neural progenitors. Nevertheless, in both progenitor cell types, protein–lipid assemblies might be the essential structural determinant in the release process of prominin-1. Collectively, these data support the concept that prominin-1-containing lipid rafts may host key determinants necessary to maintain stem cell properties and their quantitative reduction or loss may result in cellular differentiation.

INTRODUCTION

The process of cell differentiation is an important issue in stem cell biology and understanding its mechanism might allow us to manipulate the fate of primitive cells thus opening novel modalities for stem cell-based therapies. This is particularly true for haematopoietic stem and progenitor cells (HSPCs), which have the capacity to self-renew and the ability to differentiate into mature blood cells, enabling them to repopulate the bone marrow upon their clinical transplantation. The exclusion of molecular determinants necessary to maintain stem cell properties is hypothesized to be a key aspect underlying the cell differentiation mechanism, potentially leading to the differentiation process.

Thirteen years ago, a novel cholesterol (Ch)-interacting, pentaspan membrane glycoprotein, named prominin-1 (CD133) has been identified as a surface marker of both neural (Weigmann et al, 1997) and haematopoietic (Yin et al, 1997) stem and progenitor cells. Since numerous somatic stem cells and cancer stem cells originating from different organ systems have been demonstrated to express it, prominin-1 might become—among other things—a biological tool for stem cell

(1) Tissue Engineering Laboratories (BIOTEC), Technische Universität Dresden, Dresden, Germany
(2) Max-Planck-Institute of Molecular Cell Biology and Genetics, Dresden, Germany
(3) DFG Research Center and Cluster of Excellence for Regenerative Therapies Dresden (CRTD), Technische Universität Dresden, Dresden, Germany
(4) Medical Clinic and Polyclinic I, University Hospital Carl Gustav Carus, Dresden, Germany
***Corresponding author:** Tel: +49 (0) 351 463 40118,
Fax: +49 (0) 351 463 40244;
E-mail: corbeil@biotec.tu-dresden.de

†MWB, JK and A-VF should be considered joint second authors.

isolation and a molecular target for effective cancer therapies (Fargeas et al, 2006; O'Brien et al, 2007; Singh et al, 2004; Vander Griend et al, 2008). In both epithelial and non-epithelial cell types, prominin-1 is specifically localized to plasma membrane protrusions, *e.g.* microvilli (Bauer et al, 2008; Corbeil et al, 2000; Weigmann et al, 1997), by a mechanism involving Ch-based membrane microdomains (lipid rafts; Gillette et al, 2009; Röper et al, 2000). Although its physiological function in stem cells remains elusive, we have previously observed that during the cell division of neural and HSPCs prominin-1 was either symmetrically or asymmetrically distributed between the two nascent daughter cells (Bauer et al, 2008; Fargeas et al, 2006; Kosodo et al, 2004). Its association with lipid rafts, which are known to play a role in signal transduction (Simons & Toomre, 2000), is particularly interesting in this context. Prominin-1-containing lipid rafts might host key determinants or players necessary to maintain stem cell properties—their quantitative reduction or loss might result in differentiation (Fargeas et al, 2006; Marzesco et al, 2005). In agreement with this, Kosodo et al could demonstrate that neurogenic cell divisions of neural progenitors, but not proliferative ones, involve such an asymmetric distribution of prominin-1 (Kosodo et al, 2004).

Additionally, we could show that in the developing embryonic mouse brain, prominin-1 is released from neural progenitor cells into the lumen of the neural tube during the early phase of neurogenesis (Marzesco et al, 2005). Therein, prominin-1 is associated with small (50–80 nm) membrane vesicles that were distinct from exosomes and appeared to bud from microvilli and/or primary cilium (Dubreuil et al, 2007; Marzesco et al, 2005). Such prominin-1-containing membrane vesicles (prominin-1-CMV) were also found in human cerebral fluids, and remarkably appear to be up-regulated in glioblastoma patients suggesting that putative cancer stem cells might release them as well (Huttner et al, 2008).

Does a similar phenomenon exist in other stem cell type or is it unique to those derived from the neural system? Is the release of prominin-1-CMV a read out of differentiation in general? Here, we have addressed these issues using an established *ex vivo* co-culture system consisting of primary HSPCs growing on multipotent mesenchymal stromal cells (MSCs) as a feeder cell layer in a cytokine-driven protocol as a cellular model (Freund et al, 2006). Our data demonstrate that HSPCs also release prominin-1 during their differentiation but the cellular mechanism underlying it appears to be distinct from the one occurring in neural progenitors (Dubreuil et al, 2007; Marzesco et al, 2005). Finally, upon release, prominin-1-CMV could be internalized by feeder cells suggesting a potential role in intercellular communication.

RESULTS

Primary haematopoietic stem cells release prominin-1-containing membrane vesicles

To determine whether HSPCs release the stem cell marker prominin-1 as previously reported for neural progenitors (Corbeil et al, 2010), the 1-week-old conditioned co-culture HSPC/MSC medium was collected and then subjected to differential centrifugation followed by immunoblotting of the recovered pellets for prominin-1. As expected, a 120-kDa prominin-1-immunoreactive band was detected in the $300 \times g$ pellet fraction that contains prominin-1-positive HSPCs (Fig 1A, prominin-1, arrow). Interestingly, prominin-1 immunoreactivity was also observed in the $200{,}000 \times g$ pellet (Fig 1A, prominin-1, arrow). No or little immunoreactivity was detected in the other fractions, *i.e.* the 1200, 10,000 and $400{,}000 \times g$ pellet (Fig 1A, prominin-1). The association of prominin-1 with the $200{,}000 \times g$ pellet appears specific since CD34 was not detected (Fig 1A, CD34, arrowhead, $n = 3$). Upon further fractionation by equilibrium sucrose gradient centrifugation (0.1–1.2 M), the prominin-1-containing $200{,}000 \times g$ pellet (as revealed by immunoblotting) was found in a peak of relatively low buoyant density (Fig 1B, Fraction 4–6, 1.07 g/ml, arrow) similar to that of exosomes or synaptic vesicles (Huttner et al, 1983; Théry et al, 2002). Only a limited amount was detected in the pellet fraction (Fig 1B, P, arrow).

To assess the nature of the material associated with the $200{,}000 \times g$ pellet, an electron microscopy (EM) analysis was undertaken. This revealed the presence of small membrane vesicles with an approximate diameter of 40–80 nm (Fig 1C and D, arrows) and larger electron-dense membrane structures with a diameter range of 200–600 nm (Fig 1D, arrowhead). Following immunogold labelling of prominin-1, both the smaller membrane vesicles and the larger membrane structures were positive (Fig 1E). The latter may correspond to the prominin-1-immunoreactive materials found in the pellet fraction of equilibrium sucrose density gradient (Fig 1B, P). Such larger structures are similar in size to a heterogeneous microvesicle population (100 nm to 1 μm) previously described to be derived from the plasma membrane (Ratajczak et al, 2006). Not all small membrane vesicles were immunolabelled (Supporting Information Fig S1A–C). Furthermore, the material associated with $200{,}000 \times g$ pellet were positive for CD63 (Supporting Information Fig S1D), a tetraspan membrane protein highly enriched in exosomes from virtually any cell type (Théry et al, 2002), indicating the presence of such vesicles in this fraction as expected from their relative low buoyant density (see above).

We next addressed whether prominin-1 associated with $200{,}000 \times g$ pellet-derived membrane vesicles is differentially extractable in certain non-ionic detergents (Triton X-100 *vs.* Lubrol WX) as previously described for microvillar-associated ones (Röper et al, 2000) indicating its potential association with a given subset of lipid rafts (Pike, 2004). Upon lysis of whole HSPC fractions from 1-week-old co-culture with either 0.5% Triton X-100 or Lubrol WX for 30 min at 4°C, prominin-1 was found to be completely soluble in Triton X-100 after centrifugation for 1 h at $100{,}000 \times g$ (Fig 1F, Cells, Triton-100, S, arrow), while interestingly being partly insoluble in Lubrol WX (Fig 1F, Cells, Lubrol WX, P, arrow) as previously shown in epithelial cells (Röper et al, 2000). When the association of prominin-1 with detergent-resistant membrane complexes was investigated with HSPC-derived vesicles along the same lines as for the cells, a similar phenomenon could be observed (Fig 1F, $200{,}000 \times g$

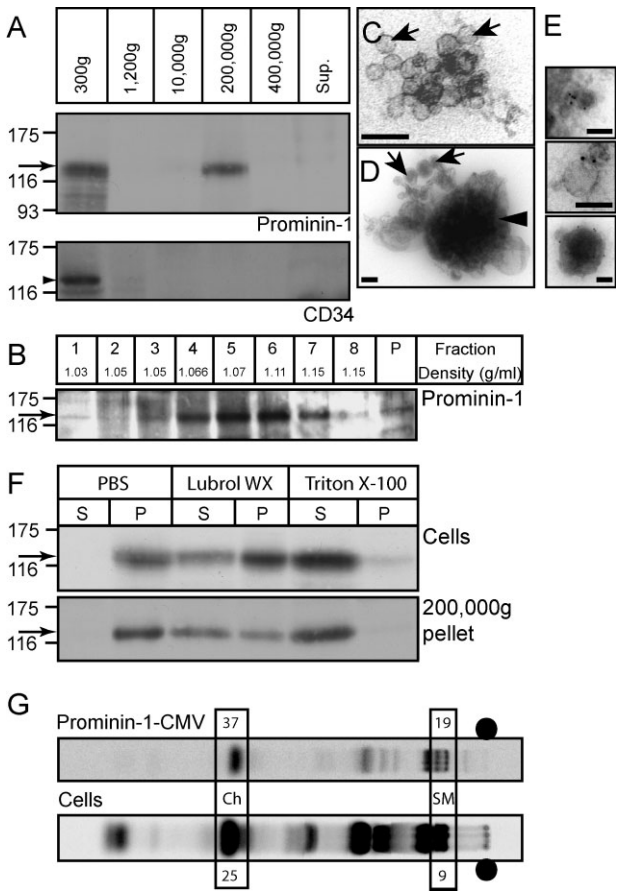

Figure 1. Association of prominin-1, but not CD34, with lipid raft-membrane vesicles released by HSPCs.

A. One-week-old co-culture HSPC/MSC conditioned medium was subjected to differential centrifugation for 5 min at 300 × *g*, 20 min at 1200 × *g*, 30 min at 10,000 × *g*, 60 min at 200,000 × *g* and 60 min at 400,000 × *g*. The resulting pellets were analysed by immunoblotting for either prominin-1 (top panel, arrow) or CD34 (bottom panel, arrowhead). Proteins in the 400,000 × *g* supernatant (Sup.) were analysed in parallel.

B. The 200,000 × *g* pellet recovered after differential centrifugation (panel A) was subjected to equilibrium sucrose gradient (0.1–1.2 M) centrifugation. Equal volumes of the recovered fractions and the pellet were analysed by immunoblotting for prominin-1 (arrow).

C,D. Negative EM analysis of the 200,000 × *g* pellet revealed the presence of small membrane vesicles (~40–80 nm; arrows) and larger dense structures (~200–600 nm; arrowhead).

E. Negative staining EM of prominin-1 immunogold-labelled membrane vesicles recovered in the 200,000 × *g* pellet. Scale bars, 100 nm [(C–E)].

F. Haematopoietic cells (Cells) growing for 1 week in the co-culture system and 200,000 × *g* pellets (200,000 × *g* pellet) recovered upon differential centrifugation (panel A) were lysed for 30 min at 4°C in either 0.5% Triton X-100 or Lubrol WX or without detergent (PBS) and centrifuged for 60 min at 100,000 × *g*. The resulting supernatants (S) and pellets (P) were analysed by immunoblotting for prominin-1 (arrows).

G. Lipid composition analysis of prominin-1-CMV was performed by C^{14}-acetate labelling of HSPCs co-cultured with MSCs followed by TLC analysis of either haematopoietic cells (Cells) or the released prominin-1-positive vesicles recovered by a paramagnetic isolation with mAb CD133 (prominin-1-CMV). Percentages of cholesterol (Ch) and sphingomyelin (SM) of the total lipid composition are indicated. •, sample loading point.

pellet, Lubrol WX, P and Triton X-100, S, arrow), indicating that prominin-1 is partly associated with Lubrol WX-insoluble membrane complexes in both HSPCs and the derived membrane vesicles. Lipid rafts are enriched in Ch and sphingomyelin (SM; Brown & London, 2000). In order to further dissect the lipid composition of prominin-1-containing HSPC-derived membrane vesicles, we analysed them by thin layer chromatography (TLC) following C^{14}-acetate labelling for 3 days. By comparison to haematopoietic cells (Fig 1G, Cells), which reveal a ~25% Ch and ~9% SM content of the total lipid composition, the prominin-1-immunoprecipitated vesicle fraction (Fig 1G, prominin-1-CMV) appears enriched in Ch and SM with ~37 and ~19%, respectively, thus indicating a distinct lipidic composition compared to the membranes of origin.

Association of prominin-1 with exosomes

To morphologically determine the source of prominin-1-CMV, we re-investigated the prominin-1 localization within the MSC-adherent HSPC population by indirect (differential) immunofluorescence microscopy. As originally described (Freund et al, 2006), the cell surface labelling revealed preferential localization of prominin-1 in various plasma membrane protrusions, *e.g.* leading edge of magnupodium or lamellipodium (Fig 2A, red, arrow). In cells with a round morphology, prominin-1 is often concentrated in one pole (Fig 2A, red, arrow)—previously described to be enriched in microvillar-like structures (Bauer et al, 2008; Freund et al, 2006). Remarkably, a second round of labelling performed upon cell permeabilization revealed an additional, intracellular staining of prominin-1 (Fig 2A, green). Thus, two distinct pools of prominin-1 molecules co-exist in haematopoietic cells. Note that in rare cases, only an intracellular or a cell surface staining of prominin-1 could be detected (Supporting Information Fig S2). To gain more insight into the intracellular pool, we double-labelled cells with different cytoplasmic organelle markers. Neither GM130, TGN46 nor BODIPY showed a significant co-localization with prominin-1 suggesting the exclusion of the latter from the *cis*-Golgi apparatus, the *trans*-Golgi network and lipid droplets, respectively (Supporting Information Fig S3). Interestingly, a partial localization of prominin-1 with either early endosomal antigen 1 (EEA1) or Smad anchor for receptor activation (SARA) could be observed (Supporting Information Fig S4), indicating that a minute fraction of prominin-1 is associated with the early and/or signalling endosomal compartment (Bökel et al, 2006). Furthermore, a significantly overlapping signal was observed with CD63 indicating the potential association of prominin-1 with exosomal-like structures (Fig 2B). To address this issue in detail, we performed an EM analysis. Surprisingly, we could visualize prominin-1 not only in plasma membrane protrusions as previously reported (Corbeil et al, 2000; Fig 2C, arrow) but also in small intraluminal membrane vesicles within multivesicular bodies (Fig 2C, see inset, arrowheads). Under our experimental conditions, not all of them were immunolabelled, which is in agreement with the data obtained with membrane vesicles found in the 200,000 × *g* pellet (Fig 1 and Supporting Information Fig S1). As expected, multivesicular bodies were labelled with an anti-CD63 antibody (Fig 2D, arrowheads).

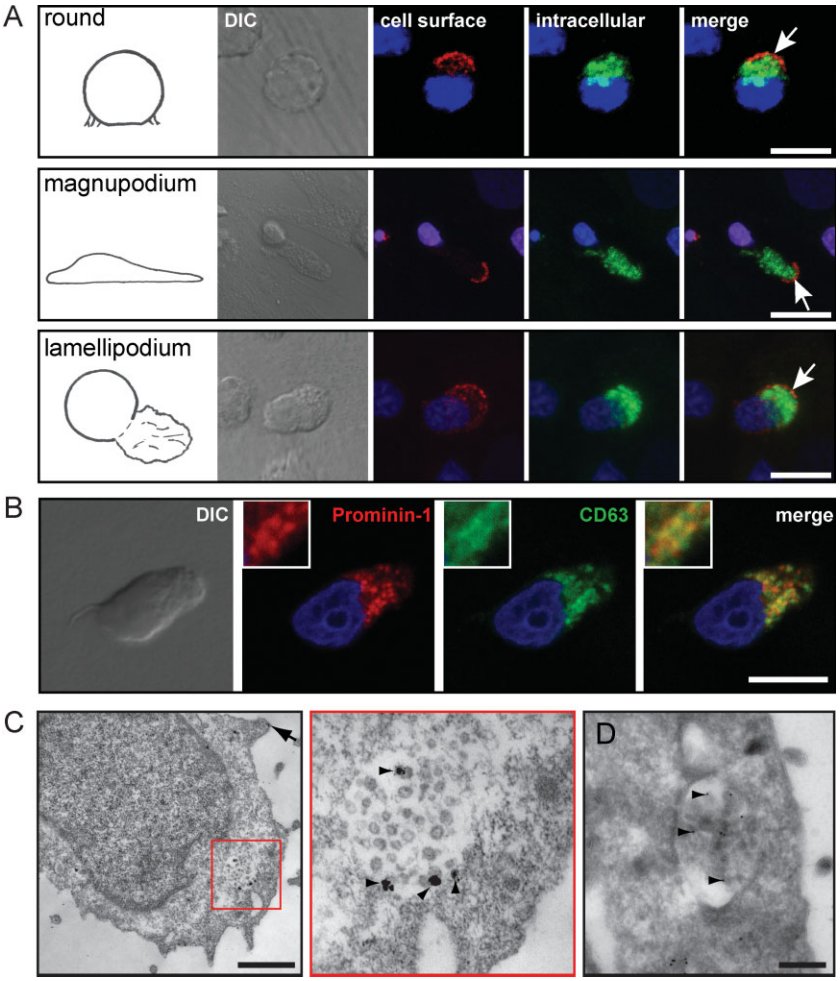

Figure 2. Two pools of prominin-1 co-exist in HSPCs.

A. HSPCs growing for 1 week on MSCs were first cell surface-labelled for prominin-1 prior to PFA fixation and saponin-permeabilization followed by a second round of prominin-1 labelling. The nuclei were stained with Hoechst (blue). The labelled cells were analysed using confocal laser scanning microscopy. A composite of 16 optical sections of HSPCs exhibiting various morphologies as indicated are shown. Note that prominin-1 is not only found at the cell surface (red, arrows) but also in intracellular compartments (green) of the HSPCs. DIC, differential interference contrast.

B. Partial co-localization of prominin-1 and endosomal/lysosomal/exosomal marker CD63. PFA-fixed, saponin-permeabilized HSPCs growing on MSCs were double-immunolabelled for prominin-1 (red) and CD63 (green) followed by appropriate secondary antibodies and observed by confocal laser scanning microscopy. Nuclei were visualized with Hoechst (blue). A single optical *x–y*-plane section revealed that prominin-1 and CD63 partially co-localized in intracellular structures. A high magnification view is shown in the corresponding inset.

C,D. Negative staining EM of prominin-1 (C) or CD63 (D) immunogold labelled HSPCs followed by silver enhancement (C) revealed the localization of prominin-1 in either small membrane vesicles present within multivesicular bodies (C, see inset, arrowheads) or microvillar-like structures present at the cell surface (C, arrow). (C) The red box in the left panel demarcates the region displayed at higher magnification in the right panel. The multivesicular bodies were also labelled with CD63 (D). Note that the membranous structures were not well preserved due to saponin-permeabilization (C) prior the labelling procedure. Scale bars, 10 μm [(A) and (B)], 0.5 μm [(C) and (D)].

In order to further elaborate on the protein composition of HSPC-derived prominin-1-positive vesicles, we performed anti-prominin-1 immuno-affinity isolation and analysed vesicle contents by immunoblotting for specific markers. Interestingly, in addition to prominin-1 (Supporting Information Fig S5; prominin-1, top panel, arrow), we could observe, three other molecules reported to be associated with exosomes; flotillin-1, flotillin-2 (Supporting Information Fig S5; middle panels, arrow) and the cytoplasmic PDZ-domain protein syntenin (Supporting Information Fig S5; bottom panel, arrow). The latter was only detectable in a limited amount in the prominin-1-positive vesicle fraction. Syntenin has been shown to be a major protein constituent of dendritic cell-derived exosomes (Théry et al, 2001).

Release of prominin-1-containing membrane vesicles during the differentiation process

Is the release of prominin-1-CMV concomitant with HSPC differentiation? To answer this question, we analysed the relative amount of prominin-1-CMV released by HSPCs with time in culture by immunoblotting (Fig 3A). HSPCs were co-cultured for 4, 9 and 14 days. Interestingly, we could observe that over different time periods, the number of prominin-1-positive HSPCs initially increased as determined by flow cytometry (from day 4 to 9; Fig 3B, prominin-1-positive HSPC), which was also reflected by prominin-1 immunoreactivity detected in $300 \times g$ pellet (Fig 3A, compare top and middle panels, respectively), and then decreased (from days 9 to 14; Fig 3B, prominin-1-positive HSPC). In parallel to this decrease, the relative amount of the prominin-1-CMV recovered in the $200{,}000 \times g$ pellet remarkably increased (Fig 3A and B, ratio of $200{,}000 \times g/300 \times g$). A similar phenomenon was observed using 5- or 10-days time windows (Fig 3C and D). In addition to the full-length prominin-1 detected in cells ($300 \times g$ pellet), but not in $200{,}000 \times g$ pellet fraction, additional faster migrating prominin-1-immunoreactive bands can be observed (Fig 3A, middle and bottom panels) suggesting its intracellular degradation. Finally, it could be observed that, in

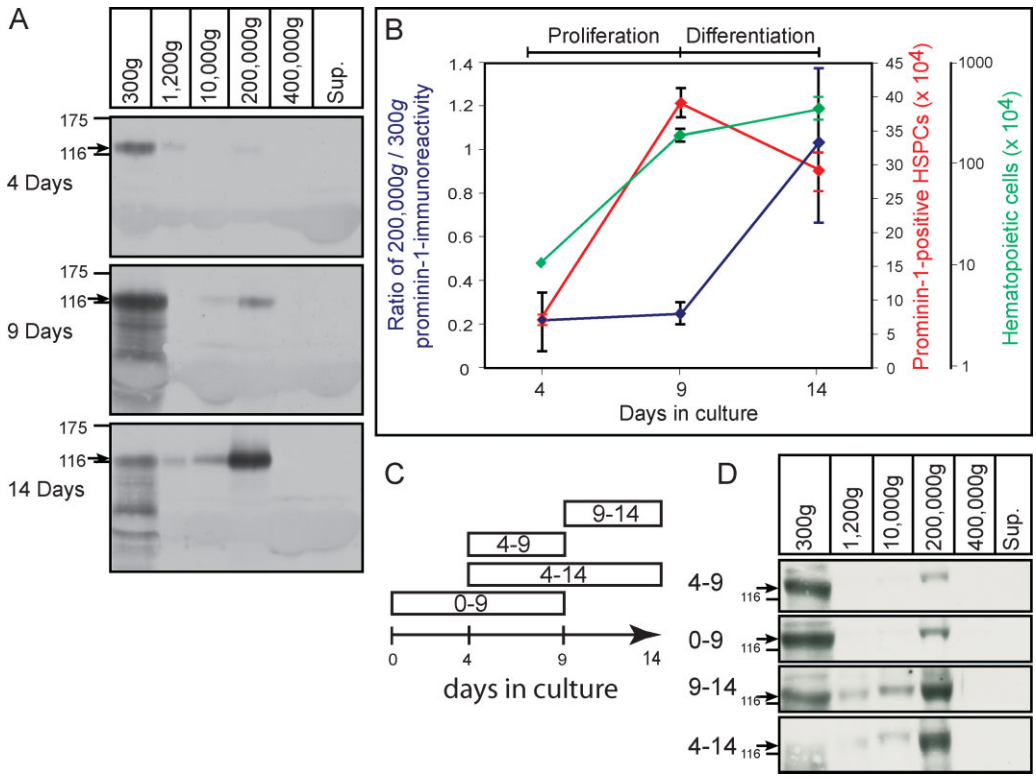

Figure 3. Release of prominin-1-containing membrane vesicles concomitant with haematopoietic stem cell differentiation.

A. Differential centrifugation of conditioned HSPC/MSC media recovered after either 4, 9 or 14 days in culture as in Fig 1A. The resulting pellets were analysed by immunoblotting for prominin-1 (arrow) using mAb 80B258 and quantified.

B. Ratio of prominin-1-immunoreactivity found in the 200,000 × *g* pellet (vesicles) *versus* the 300 × *g* pellet (cells) were plotted for the 4, 9 and 14 days of culture (left *y*-axis; blue). Total number of haematopoietic cells and prominin-1-positive HSPCs present in culture after 4, 9 and 14 days were indicated in the right *y*-axes, green and red, respectively ($n = 4$). The number of prominin-1-positive cells was calculated by multiplying the percentage of prominin-1-positive cells (observed by FACS analysis) with the total number of cells. Note that the general proliferation of prominin-1-positive HSPCs stops after 9 days in culture.

C. Summary of the different conditions. Conditioned media from HSPCs growing on MSCs were recovered after 5 (conditions 4–9 or 9–14) or 10 (conditions 0–9 or 4–14) days in culture. The new medium was added to day 0 (plating day; condition 0–9) or to the 4- (conditions 4–9 and 4–14) or 9- (condition 9–14) days old cultured cells.

D. Differential centrifugation of conditioned media obtained from the four culture conditions described in (C). The resulting pellets were analysed as in (A).

parallel to the decreasing level of prominin-1 in HSPCs, the relative expression of differentiation markers such as CD42b and CD61 increased (Fig 4). Under these culture conditions less than 2% (*i.e.* after 9 days, 0%; after 14 days, 2%; $n = 320$ cells) prominin-1-positive HSPCs stained positive for annexin V indicating that apoptosis is not the underlying mechanism of the release of prominin-1-CMV, which is in line with the general resistance of prominin-1-positive cells to apoptosis (Chiou et al, 2008; Zobalova et al, 2008).

Could we provoke the release of prominin-1-CMV? We have addressed this question by stimulating HSPC differentiation using phorbol esters such as phorbol 12-myristate 13-acetate (PMA) as previously reported (Rossi et al, 1996). HSPCs cultivated on MSCs for only 2 days were exposed for 3 additional days to 160 nM PMA prior to differential centrifugation. Interestingly, the amount of prominin-1 immunoreactivity recovered in the 200,000 × *g* pellet fraction (vesicles) significantly increased under differentiation condition, whereas, its fraction in the 300 × *g* pellet (cells) decreased (Fig 5, panel A *vs.* panel B). In contrast to prominin-1, neither actin nor α-tubulin were recovered in the 200,000 × *g* pellet (Fig 5), which rules out both fragmentation of plasma membrane protrusions (*e.g.* actin-based microvillus) and relics of cytokinesis (tubulin-based) in this fraction. The very small amount of prominin-1 in the 1200 and 10,000 × *g* pellets might nevertheless derive from such membranes (see also Fig 3A; Dubreuil et al, 2007; Giebel & Beckmann, 2007). Similar results were obtained when HSPCs were growing on a fibronectin-coated plastic surface instead of MSCs thus excluding potential side effects of feeder cells (Fig 5A and B). In parallel, the differentiation of HSPCs induced by PMA was monitored based on the expression of typical stem or differentiated CD markers using either microscopy or flow cytometry (for details see Legend of Supporting Information Fig S6). As expected, the number of prominin-1-positive cells decreases after PMA treatment (Supporting Information Fig S6C, CD133; see also Fig 6C).

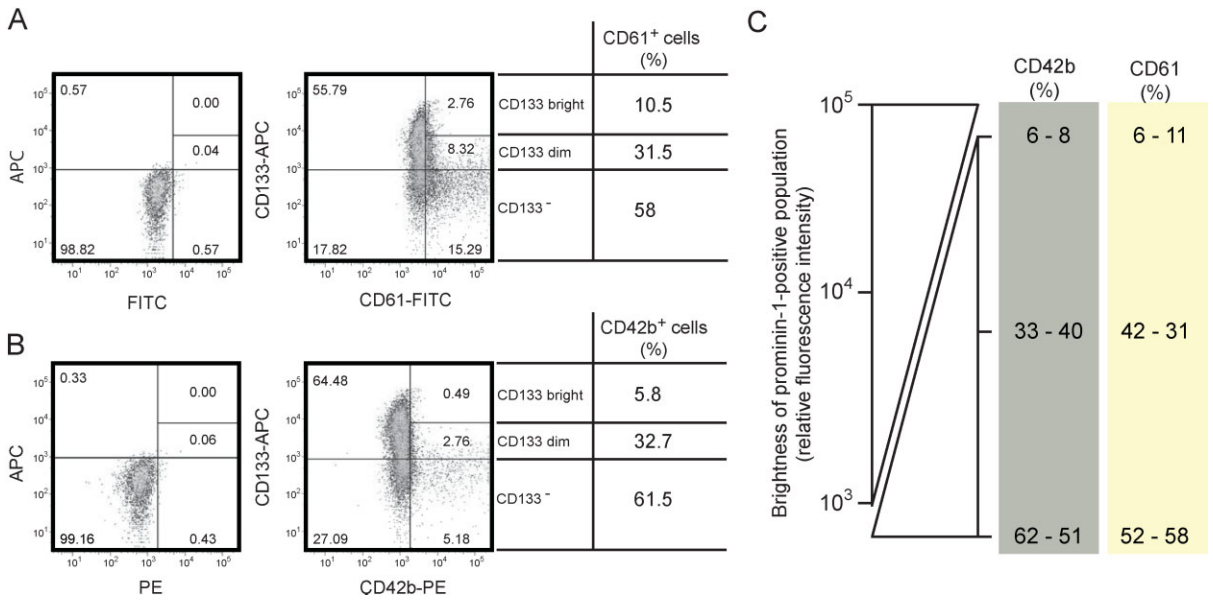

Figure 4. Expression of prominin-1 *versus* either CD61 or CD42b.

A,B. Flow cytometric analysis revealed phenotypes of HSPCs cultured for 1 week on MSCs for the expression of prominin-1 (CD133) *versus* either CD61 (A) or CD42b (B). The gates were set according to unstained cells and isotype controls (left panels). The amount of CD133-bright, -dim and -negative cell population is shown as a percentage of the whole CD61- or CD42b-positive population (right panels).

C. The percentage of cells harbouring the differentiation markers CD61 and CD42b increased concomitant with the decrease in prominin-1 (CD133) expression, resolving that they are mainly expressed on prominin-1-negative cell population. Data obtained from two independent experiments are shown.

Remarkably, concomitant with PMA-induced HSPC differentiation we could observe two phenomena by indirect (differential) immunofluorescence microscopy for prominin-1 (Fig 6). First, in some cells, the cell surface pool of prominin-1 is slightly increased (Fig 6A, PMA, left panel, red), which was quantified using flow cytometry by an increase of median fluorescence intensity (MFI; Fig 6C). The contact of multivesicular bodies with the plasma membrane might explain this phenomenon. Second, the intracellular pool of prominin-1 was significantly depleted (Fig 6A, PMA, green) in comparison to the untreated ones (Fig 6A, control, green) as quantified by a net reduction of the ratio intracellular *versus* surface staining (Fig 6D). Such events were also observed after only 1 day of PMA treatment (Fig 6B and D). These observations are in line with early data showing the release of exosomes upon phorbol ester treatment of Daudi cells (Clayton et al, 2001). Collectively, the present data indicate that the stem cell marker prominin-1 is released and/or degraded by HSPCs concomitant with their differentiation.

Prominin-1-containing membrane vesicles are transferred to feeder cells

It becomes more and more evident that exosome-like vesicles released by various cell types can mediate the transfer of biochemical information between cells (Simons & Raposo, 2009). Do prominin-1-CMV shuttle between cells? Technically, we have addressed the latter issue by labelling the prominin-1-CMV with a membrane dye and following their potential uptake by either MSCs or HSPCs. Interestingly, after 6 h of incubation we could observe DiO-labelled prominin-1-CMV inside MSCs where they partly co-localized with SARA indicating their intracellular delivery to the endosomal compartment of recipient cells (Fig 7, top panels). Such internalization was not observed after 1 h of incubation as DiO-labelled-vesicles were detected solely at the cell surface of hosts (Fig 7, middle panels). Surprisingly, we could not observe such phenomenon with neighbouring HSPCs as recipient cells suggesting the selectivity of the transfer processes (Fig 7, bottom panels, asterisks). However, we could not formally exclude that in the latter cell type a rapid degradation of prominin-1-CMV occurs.

DISCUSSION

Intriguingly, we demonstrated that, in contrast to other prominin-1-expressing cell types studied so far, *e.g.* epithelial cells (Karbanová et al, 2008; Weigmann et al, 1997), HSPCs contain an important intracellular pool of prominin-1 in addition to the cell surface one. Inside the cell, prominin-1 is located primarily in membrane vesicles within multivesicular bodies. The exosomal localization of prominin-1 is supported by (i) its presence in low-buoyant density sucrose fractions (1.05–1.15 g/ml) as reported for exosomes (Théry et al, 2002), (ii) its partial co-localization with CD63, (iii) electron microscopic analysis and (iv) the presence of the exosomal markers flotillins and syntenin in prominin-1-CMV. Few reports have mentioned the presence of prominin-1 within the intracytoplasmic compartment of cancerous and/or transformed cells such as adenocarcinoma-derived epithelial Caco-2 cells (Corbeil et al, 2000;

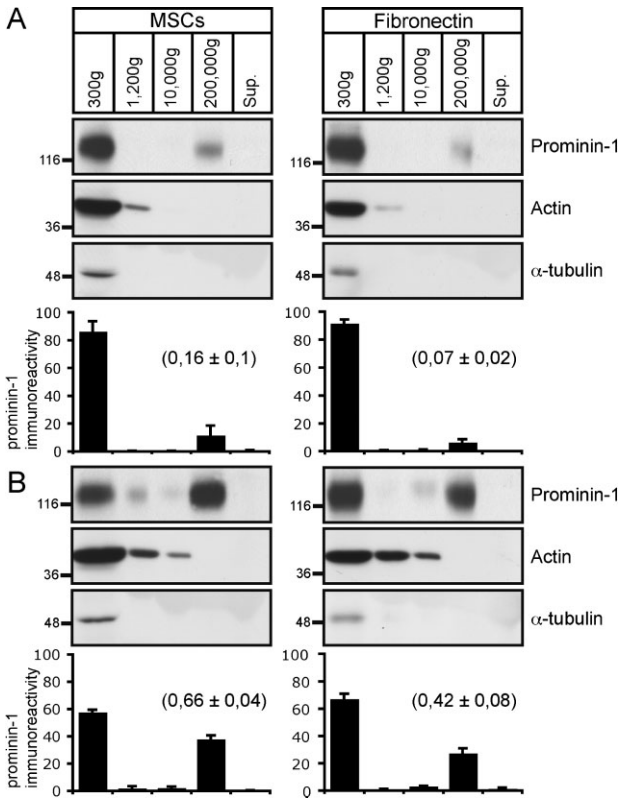

Figure 5. Provoked differentiation stimulated prominin-1-containing membrane vesicle release.

A,B. HSPCs pre-cultured either on MSCs or fibronectin-coated dishes for 2 days were incubated in the absence (A) or presence (B) of PMA. After 3 days, conditioned media were subjected to differential centrifugation as in Fig 1A. The resulting pellets were analysed by immunoblotting for prominin-1, actin and α-tubulin. Note that only 1/3 of materials were loaded for the 300 × *g* fraction. The amount of prominin-1 immunoreactive materials was quantified [$n = 3$ (MSCs) and 4 (fibronectin)]. Results are the mean ± SEM. Ratio of prominin-1-immunoreactivity found in the 200,000 × *g* pellet (vesicles) *versus* 300 × *g* (cells) is indicated in bracket. Note that the provoked HSPC differentiation triggered by PMA resulted in an increase of prominin-1 in 200,000 × *g* pellets, which are devoid of cytoskeletal proteins under both culture conditions.

Immervoll et al, 2008). The latter example is particularly interesting since the release of prominin-1-CMV from these cells has been reported solely during the process of and upon differentiation (Marzesco et al, 2005) by a mechanism involving lipid rafts (Marzesco et al, 2009). Given that HSPCs harbour few microvillar-like structures in contrast to epithelial cells such as neural progenitors (Corbeil et al, 2000; Weigmann et al, 1997), but numerous multivesicular bodies, the endocytic–exocytic pathway may represent the major way for the release of prominin-1 in non-epithelial stem and progenitor cells.

In agreement with the detergent-resistance extraction observed for prominin-1 within released membrane vesicles as well as the lipid raft—association of two other molecules found therein, *i.e.* flotillin-1 and flotillin-2 (de Gassart et al, 2003; Rajendran et al, 2003; Salzer & Prohaska, 2001; Staubach et al, 2009), it appears that specific lipid–protein interactions might act as a platform for either the exosomal targeting or the extracellular release of the prominin-1-containing exosomes. Both scenarios are not mutually exclusive, and the direct interaction of prominin-1 with membrane Ch is consistent with it (Röper et al, 2000). These observations are coherent with recent data demonstrating that lipid rafts may participate in the exosomal protein sorting independently of endosomal sorting complex required for transport (ESCRT) machinery (Trajkovic et al, 2008). A full molecular characterization of prominin-1-containing exosomes described here and determination of exosomal targeting mechanism(s) of prominin-1 should answer these open issues.

Taken together, the release of prominin-1-containing exosomes concomitant with cellular differentiation may represent an alternative mechanism of externalization of stem/progenitor properties-containing lipid rafts, in addition to the budding mechanism underlying the release of prominin-1 from plasma membrane protrusions (*i.e.* microvillus and primary cilium) of neural progenitors (Corbeil et al, 2010; Dubreuil et al, 2007; Marzesco et al, 2005, 2009). Thus, the concept of '*stem cell-specific lipid rafts*' holding molecular determinants necessary to maintain the stem cell properties is attractive in this context (Fargeas et al, 2006; Marzesco et al, 2005) and the characterization of those containing prominin-1 including their proteome and lipidome may reveal new aspects of stem cell biology. Along the same line, it will be of interest to determine whether similar phenomena occur in cancerous tissues [other than the brain (Huttner et al, 2008)] given that the expression of prominin-1 is often associated with transformed, treatment-resistant cells exhibiting tumour-initiating properties (Bao et al, 2006; Liu et al, 2006).

Lastly, we could demonstrate the internalization of prominin-1-CMV by feeder cells suggesting an additional function in intercellular communication either by stimulating target cells as signalling devices via cell surface expressed ligands or by transferring surface receptors/adhesion molecules or small RNA between cells (Bakhti et al, 2011; Eldh et al, 2010; Janowska-Wieczorek et al, 2001; Ratajczak et al, 2006). Such a phenomenon is in line with exosome-like vesicles acting as vesicular carriers for intercellular communication (Simons & Raposo, 2009; Théry et al, 2009). Again, additional investigation is urged to reveal whether prominin-1-CMV modify the biochemistry of the recipient MSCs (Freund et al, 2010) as it was elegantly proposed upon the direct contact of HSPCs with osteoblasts (Gillette et al, 2009). Thus, the intercellular communication of HSPCs with their bone marrow microenvironment is a novel research field that requires further investigation (Méndez-Ferrer et al, 2010) and the development of animal models to demonstrate its *in vivo* impact.

In conclusion, we have highlighted that during the process of differentiation, HSPCs release prominin-1-CMV, which are then internalized by feeder cells.

MATERIALS AND METHODS

Primary cells and cultivation

Primary HSPCs and MSCs were collected from healthy donors after informed consent and approval of the local ethics committee. The

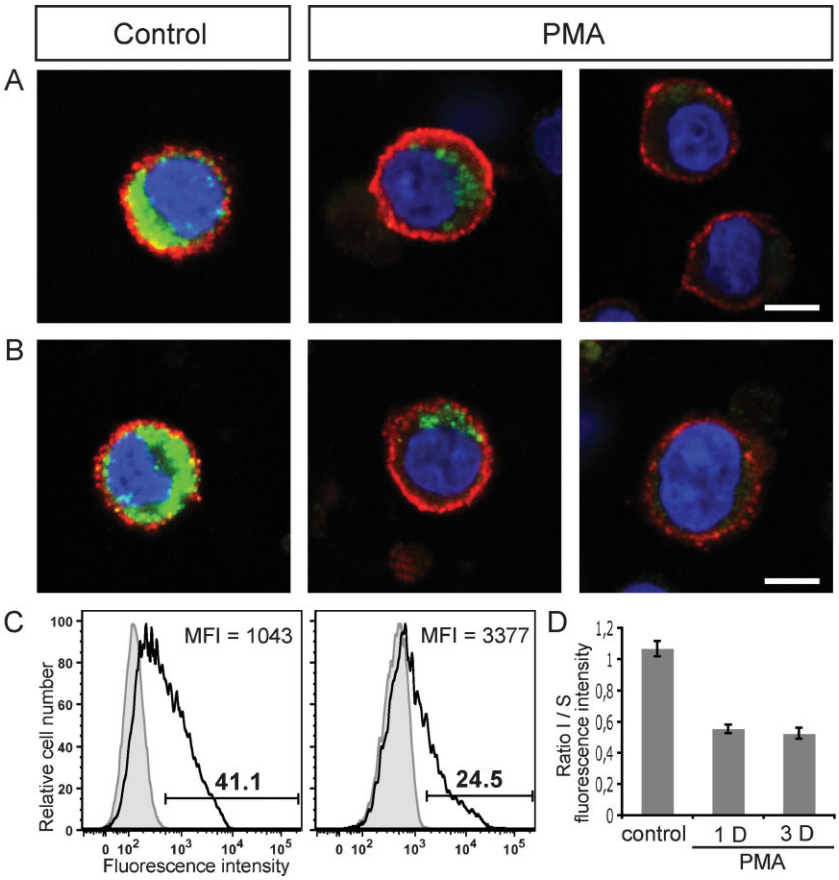

Figure 6. Intracellular pool of prominin-1 is depleted upon PMA treatment.

A,B. HSPCs pre-cultured on MSCs for 2 days were incubated in the absence (control) or presence of phorbol ester PMA (PMA). After 3 (A) or 1 (B) days, cells were first cell surface-labelled for prominin-1 (red) prior to PFA-fixation and saponin-permeabilization followed by a second round of prominin-1 (green) labelling. The nuclei were stained with DAPI (blue). The labelled cells were analysed using confocal laser-scanning microscopy. A single optical *x*–*y*-plane section is shown. Scale bar, 5 μm [(A) and (B)].

C. After 3 days of incubation without (left panel) or with (right panel) PMA the number (indicated above the bar) of prominin-1-positive cells (open areas) was reduced, whereas, the MFI was slightly increased as analysed by flow cytometry. Appropriate isotype-matching control is depicted (grey filled areas).

D. The ratio of intracellular (I) *versus* cell surface (S) fluorescence intensity of prominin-1 was quantified using CellProfiler 2.0 software. Results are the mean ± SEM. ($n = 60$ cells; three independent donors). Note the reduction of the intracellular pool of prominin-1 upon 1 or 3 days (D) of PMA treatment.

isolation of both cell types was performed as described (Freund et al, 2006). CD34+ MACS-immuno-isolated HSPCs from leukapheresis products were cultured on MSCs growing on various supports in serum-free medium supplemented with early acting cytokines (stem cell factor, foetal liver tyrosine kinase-3 ligand and interleukin-3; IL-3). Unless otherwise stated, HSPCs/MSCs were incubated at 37°C in a humidified 5% CO_2 atmosphere for 7 days before use. For the PMA treatment, HSPCs pre-cultured for 2 days on either MSCs or directly on fibronectin-coated six-well plates were incubated in medium containing 160 nM of PMA for 3 additional days. Alternatively, HSPCs were pre-cultured for 4 days before 1 day of PMA treatment.

Differential centrifugation and detergent lysis

Conditioned HSPC/MSC medium was subjected to differential centrifugation as follows: 5 min at 300 × *g*; supernatant, 20 min at 1200 × *g*; supernatant, 30 min at 10,000 × *g*; supernatant, 1 h at 200,000 × *g*; supernatant and 1 h at 400,000 × *g*. The resulting pellets were resuspended in Laemmli buffer and analysed by immunoblotting. An aliquot (1/10th) of the 400,000 × *g* supernatant was analysed in parallel. In some experiments, HSPCs and the 200,000 × *g* pellet recovered after differential centrifugation were lysed for 30 min in ice-cold buffer A (150 mM NaCl, 2 mM EGTA, 50 mM Tris–HCl pH 7.5, 10 μg/ml aprotinin, 2 μg/ml leupeptin and 1 mM PMSF) containing either 0.5% Triton X-100 or Lubrol WX (Serva). Detergent lysates were centrifuged at 4°C for 1 h at 100,000 × *g*. The entire supernatant and pellet were analysed by immunoblotting.

Sucrose gradient centrifugation

The 200,000 × *g* pellet was resuspended in phosphate buffered saline (PBS) containing 1 mM $CaCl_2$, 0.5 mM $MgCl_2$ and protease inhibitors (Complete, Roche Diagnostics), placed on top of a equilibrium sucrose gradient (0.1–1.2 M) and centrifuged at 65,000 × *g* for 5 h (Huttner et al, 1983). After centrifugation, 500 μl fractions were collected from the top to the bottom of the gradient and the pellet was resuspended in 500 μl buffer A containing 1% Triton X-100. Four hundred and fifty microlitres of aliquots of each fraction were concentrated using methanol/chloroform precipitation and analysed by immunoblotting. The remaining 50-μl aliquot of each fraction was used to determine the sucrose concentration by refractive index.

Immuno-isolation of prominin-1-containing membrane vesicles

The immuno-isolation of prominin-1-CMV was performed using immunomagnetic beads (Miltenyi Biotec, Bergisch Gladbach, Germany). The conditioned medium collected from either HSPCs growing on MSCs or, as control, MSCs alone was centrifuged at 1200 × *g* for 20 min to remove cells. Supernatants were concentrated to 400 μl by Centricon PL-30 (Millipore Corp., Belford, MA) and 400 μl of ice-cold PBS were added followed by centrifugation at 10,000 × *g* for 30 min. The 10,000 × *g* supernatants were pre-incubated with goat-anti-mouse IgG-magnetic-beads (Miltenyi Biotec) for 1.5 h at 4°C. The supernatants were then applied to ice-cold PBS conditioned MS-columns (Miltenyi Biotec) placed into a magnetic field, and the flow-

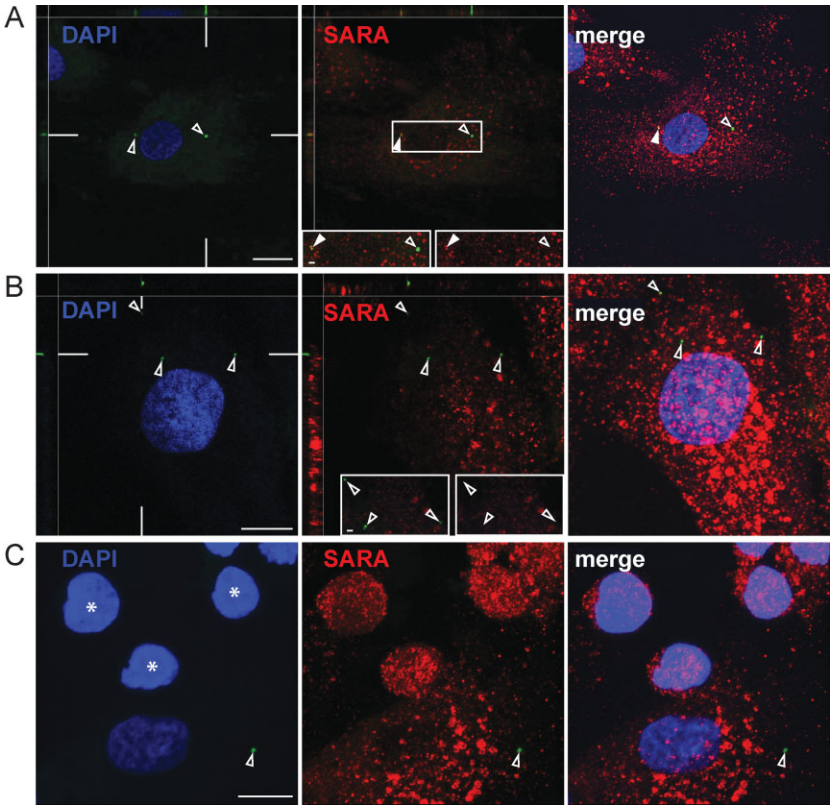

Figure 7. Internalization of prominin-1-containing membrane vesicles by feeder cells.
A,B,C. Immuno-isolated prominin-1-CMV were labelled with the membrane dye DiO (green), and then incubated with HSPC/MSC co-culture for 6 h (A and C) or 1 h (B). PFA-fixed, saponin-permeabilized cells were immuno-labelled for Smad anchor for receptor activation protein (SARA; red). Nuclei were visualized with DAPI (blue). The labelled cells were analysed using confocal laser-scanning microscopy. Single optical *x*–*y*-plane sections (A and B; DAPI and SARA) or composite of >10 sections (A and B, merge panels; C) are shown. The position of *x*–*z* sections is indicated by white lines in the corresponding panel. Insets (A and B) are displayed either in double (left) or single (right) channel. Open arrowheads, prominin-1-CMV; filled arrowheads, double-positive (prominin-1-CMV, SARA) structures; asterisks, HSPCs. Scale bars, 10 μm [(A–C)], 1 μm [(A, inset), (B, inset)].

through material was collected. Half of the HSPC/MSC medium fraction and the control fraction were then incubated each with mouse mAb CD133-magnetic-beads (Miltenyi Biotec). The other half of HSPC/MSC medium fraction was incubated with goat anti-mouse IgG-magnetic-beads as an additional control. After 1 h incubation, samples were subjected to a magnetic separation. Vesicles retained in the MS-columns were eluted by taking out the column from the magnet, and flushing with PBS. Laemmli buffer (4×) was added and the samples were stored at −20°C. The recovered flow-through fractions were centrifuged at 200,000 × *g* for 1 h to obtain the unbound materials, which were resuspended in Laemmli buffer and stored at −20°C.

SDS–PAGE and immunoblotting

Proteins were analysed by SDS–PAGE and transferred to poly(vinylidene difluoride) membranes (Millipore Corp.; Corbeil et al, 2001). Immunoblotting was performed using distinct primary antibodies followed by appropriate horseradish peroxidase-conjugated secondary antibody. Immune complexes were detected using enhanced chemiluminescence (Amersham Biosciences) and quantified after scanning the Hyperfilm (Amersham) using the MacBas or ImageJ software.

Radioactive labelling, lipid extraction and thin layer chromatography

Six-days-old HSPCs cultured on MSCs were collected and centrifuged at 1200 × *g* for 5 min. Cells were resuspended and replated onto the same MSCs in fresh HSPC medium containing 10 μCi C^{14}/100-mm Petri dish. The cells were cultured for 3 additional days. Lipids from haematopoietic cells and immunomagnetic-isolated prominin-1-CMV were extracted as follows: cells and the prominin-1-containing vesicle fractions were each put into 2 ml of MeOH/$CHCl_3$ (2:1), mixed, and centrifuged for 5 min at 3200 × *g*. The supernatants were transferred to a fresh tube, to which 0.5 ml of 20 mM acetic acid and 0.5 ml of $CHCl_3$ were added, mixed and centrifuged again for 2 min at 3200 × *g*. The lower phase was transferred to another tube, while 25 μl of 1 M citric acid and 1 ml of $CHCl_3$ were added to the upper phase, mixed and centrifuged for 2 min at 3200 × *g*. The lower phase was transferred to the same tube as the previous lower phase and the $CHCl_3$ was evaporated under a stream of nitrogen. Dried lipids were dissolved in MeOH/$CHCl_3$ (1:2) and applied to silica TLC plates (Merck) using a capillary. To separate the lipids, the plates were run in chloroform/ethanol/water/triethylamine (35:50:10:35) until 2:3 of the distance, then the plates were dried and subsequently placed and run in iso-hexane/ethylacetate (5:1) for the full distance and dried again. TLC plates were exposed to image plates (Fuji), which were analysed by the BAS 1800 II phosphoimager. Bands were identified by comparison with lipid standards and quantified using ImageGauge V4.23.

Immunofluorescence and confocal microscopy

One-week-old co-cultured HSPCs/MSCs were gently washed with PBS, fixed with 4% paraformaldehyde (PFA), quenched with 50 mM NH_4Cl and then permeabilized with 0.2% saponin in blocking buffer (PBS containing 2% foetal calf serum; FCS). Cells were sequentially incubated for 30 min with mouse mAb CD133/1 (anti-prominin-1; Miltenyi Biotec) at room temperature (RT) followed by 1 h incubation with Cy™3-conjugated AffiniPure donkey-α-mouse IgG (H + L) Fab fragment (Jackson ImmunoResearch Laboratories) at 4°C. Remaining

The paper explained

PROBLEM:

The process of cell differentiation is a central issue in stem cell biology and understanding its mechanism might allow us to manipulate the fate of stem cells opening novel avenues for stem cell-based therapies. It is equally important to understand all cellular events occurring within the stem cell niche including intercellular communication. Here, we have addressed these issues by tracking the transport of the stem cell marker prominin-1. The medical interest in this molecule has grown extremely rapidly since its cell surface appearance allows the isolation of stem cells from various organs including those derived from haematopoietic and neural systems.

RESULTS:

Using an *ex vivo* co-culture system consisting of human primary HSPCs growing on multipotent MSCs as a feeder cell layer, we describe that during the process of differentiation, the haematopoietic progenitors release small membrane vesicles containing prominin-1 by exportation via exosomes. Upon release, prominin-1-containing membrane vesicles are internalized by feeder cells.

IMPACT:

We have highlighted the role of the endocytic–exocytic pathway in the release of prominin-1, which occurs concomitantly with cellular differentiation. Such valuable information might help us in the near future to modulate the fate of rare stem cells (*e.g.* those derived from cord blood), which are clinically important. Moreover, our observations provide evidence for the intercellular communication between stem cells and their supporting feeder cells, which opens a novel research field that requires further investigation.

mouse epitopes were saturated by incubation with unconjugated AffiniPure rabbit-α-mouse IgG (H + L) Fab fragment (Jackson ImmunoResearch). After a post-fixation step with 0.2% PFA and quenching, cells were incubated for 30 min with mouse mAb MX-49.129.5 (anti-CD63; Santa Cruz Biotechnology) followed by Cy™2-conjugated goat-α-mouse antibody IgG (H + L; Jackson ImmunoResearch) at RT. In the case of cell surface *versus* intracellular labelling, cells were first cell surface labelled with mAb CD133/1 in the cold prior fixation, as described (Corbeil et al, 1999), followed by the saturation of remaining mouse epitopes with unconjugated AffiniPure rabbit-α-mouse IgG (H + L) Fab fragment. Afterward, cells were post-PFA-fixed, saponin-permeabilized and finally labelled with mAb CD133/1 as described above for anti-CD63. Alternatively, fixed, saponin-permeabilized cells were sequentially incubated for 30 min at RT with mouse mAb CD133/1 alone or with either sheep antiserum against TGN46 (Serotec) or rabbit antiserum against GM130 (Abcam) or rabbit antiserum against SARA (Santa Cruz Biotechnology) or rabbit antiserum against EEA1 (a generous gift from Marino Zerial, MPI-CBG) followed by appropriate secondary antibodies; Cy™2/3-conjugated goat anti-mouse IgG (H + L) alone or with either Cy™2-conjugated donkey anti-sheep IgG (H + L) or Cy™2/3-conjugated goat anti-rabbit IgG (H + L; Jackson ImmunoResearch). Alternatively, CD133-labelled cells were co-stained with BODIPY 493/503 (Invitrogen Molecular Probes, USA).

In all cases, nuclei were labelled with either Hoechst 33258 (Invitrogen, Karlsruhe, Germany) or 4,6-diamidino-2-phenylindole (DAPI; Molecular Probes). The cells were mounted in Mowiol 4.88. Images were captured using confocal microscope. The images shown were prepared from the confocal data files using Adobe Photoshop software. Ratio of intracellular *versus* surface immunofluorescence of prominin-1 was calculated from total image pixel intensity using CellProfiler 2.0 software (Broad Institute, Cambridge, MA).

Immunoelectron microscopy

Membrane vesicles—The 200,000 × *g* pellet was resuspended in 4% PFA in phosphate buffer and applied onto 400-mesh grids with formvar- and carbon-coating. The samples were blocked with 0.1% glycin in PBS and twice with 0.2% gelatine, 0.5% bovine serum albumin in PBS (PBG). The grids were incubated with either mAb AC141 (Miltenyi Biotec) directed against human prominin-1 or mAb PeliCluster CD63 (Sanquin) followed by goat anti-mouse IgG coupled to 10-nm gold (British Biocell). The grids were post-fixed in 2% glutaraldehyde (GA) in PBS, negatively contrasted and viewed in a Morgagni electron microscope (FEI Company). Micrographs were taken with a MegaviewII camera and AnalySIS software (Soft Imaging Systems).

HSPCs—HSPC/MSC co-cultures grown on Transwell filters were fixed with 4% PFA in PBS, quenched and then permeabilized and blocked with 0.2% saponin, 2% FCS in PBS (blocking solution). Cells were incubated with mAb CD133/1 followed by goat anti-mouse secondary antibody coupled to ultra-small gold (Aurion, Wageningen, The Netherlands). Filters were rinsed sequentially with blocking solution and PBS followed by fixation in 2% GA. The samples were processed for silver enhancement using R-GENT SE-EM silver enhancement kit (Aurion) prior to post-fixation in 1% osmium tetroxide. Dehydration was performed by a graded series of ethanol. Samples were infiltrated in EMBed resin (Science Services). Ultrathin sections were cut on a UCT ultra-microtome (Leica Microsystems) and post-stained with uranyl acetate and lead citrate. For the CD63 labelling, ultrathin cryosections were prepared as described (Dubreuil et al, 2007), and immunolabelled with mAb PeliCluster CD63.

Flow cytometry

HSPCs recovered by centrifugation were processed for flow cytometry using various antibodies (see Materials and Methods Section of

Supporting Information). Samples were analysed by acquiring 10,000 events on a FACS LSR II (BD Biosciences). Instrument settings and gating strategies were established using appropriate controls, and data were analysed using either DIVA software (BD Biosciences) or FlowJo software (TreeStar, Ashland, USA).

Double labelling of HSPCs for annexin V and prominin-1

HSPCs recovered by centrifugation were incubated with annexin V-APC (BD Bioscience), fixed with 4% PFA, quenched and blocked with blocking buffer (see above). Cells were labelled with mAb CD133/1 followed by incubation with Cy^{TM}3-conjugated goat anti-mouse IgG (H + L). Nuclei were visualized with Hoechst 33258. Cells were mounted in Mowiol 4.88 and observed on a Zeiss LSM 510 Meta microscope. The numbers of annexin V-positive cells, CD133-positive and double-positive cells were scored.

Internalization of prominin-1-containing membrane vesicles

The materials recovered in 200,000 × *g* fraction were resuspended in PBS and incubated with 3,3′-dioctadecyloxacarbocyanine perchlorate (DiO; Vybrant Cell-Labeling Solution, Molecular Probes). Afterward, DiO-labelled vesicles were immuno-isolated based on prominin-1 as described above. Isolated DiO-labelled prominin-1-CMV were incubated either for 1 or 6 h with co-cultured HSPCs/MSCs growing on fibronectin-coated coverslips. Samples were processed for immunofluorescence for SARA, and observed using a Leica SP5 upright confocal microscope.

Author contributions

NB designed experiments, performed most of the experimental work and co-wrote the manuscript; MWB performed EM analyses; JK performed PMA experiments; A-VF performed FACS analyses; DS performed SARA labelling experiments and internalization assay; DF performed annexin labelling; CT and WBH helped to design some experiments; MB provided primary cells and helped to design some experiments; DC designed experiments, supervised the project and wrote the manuscript.

Acknowledgements

Deutsche Forschungsgemeinschaft financially supported CT (TRR83 #12), MB (SFB655 B2), WBH (TRR83 #6; SFB655 A2) and DC (TRR83 #6; SFB655 B3 and CO298/5-1).

Supporting Information is available at EMBO Molecular Medicine online.

The authors declare that there is no conflict of interest.

For more information

Denis Corbeil's web page:
http://www.biotec.tu-dresden.de/research/corbeil/

References

Bakhti M, Winter C, Simons M (2011) Inhibition of myelin membrane sheath formation by oligodendrocyte-derived exosome-like vesicles. J Biol Chem 286: 787-796

Bao S, Wu Q, McLendon RE, Hao Y, Shi Q, Hjelmeland AB, Dewhirst MW, Bigner DD, Rich JN (2006) Glioma stem cells promote radioresistance by preferential activation of the DNA damage response. Nature 444: 755-760

Bauer N, Fonseca AV, Florek M, Freund D, Jászai J, Bornhäuser M, Fargeas CA, Corbeil D (2008) New insights into the cell biology of hematopoietic progenitors by studying prominin-1 (CD133). Cells Tissues Organs 188: 127-138

Bökel C, Schwabedissen A, Entchev E, Renaud O, González-Gaitán M (2006) Sara endosomes and the maintenance of Dpp signaling levels across mitosis. Science 314: 1135-1139

Brown DA, London E (2000) Structure and function of sphingolipid- and cholesterol-rich membrane rafts. J Biol Chem 275: 17221-17224

Chiou SH, Kao CL, Chen YW, Chien CS, Hung SC, Lo JF, Chen YJ, Ku HH, Hsu MT, Wong TT (2008) Identification of CD133-positive radioresistant cells in atypical teratoid/rhabdoid tumor. PLoS One 3: e2090

Clayton A, Court J, Navabi H, Adams M, Mason MD, Hobot JA, Newman GR, Jasani B (2001) Analysis of antigen presenting cell derived exosomes, based on immuno-magnetic isolation and flow cytometry. J Immunol Methods 247: 163-174

Corbeil D, Röper K, Hannah MJ, Hellwig A, Huttner WB (1999) Selective localization of the polytopic membrane protein prominin in microvilli of epithelial cells—a combination of apical sorting and retention in plasma membrane protrusions. J Cell Sci 112: 1023-1033

Corbeil D, Röper K, Hellwig A, Tavian M, Miraglia S, Watt SM, Simmons PJ, Peault B, Buck DW, Huttner WB (2000) The human AC133 hematopoietic stem cell antigen is also expressed in epithelial cells and targeted to plasma membrane protrusions. J Biol Chem 275: 5512-5520

Corbeil D, Fargeas CA, Huttner WB (2001) Rat prominin, like its mouse and human orthologues, is a pentaspan membrane glycoprotein. Biochem Biophys Res Commun 285: 939-944

Corbeil D, Marzesco AM, Wilsch-Bräuninger M, Huttner WB (2010) The intriguing links between prominin-1 (CD133), cholesterol-based membrane microdomains, remodeling of apical plasma membrane protrusions, extracellular membrane particles, and (neuro)epithelial cell differentiation. FEBS Lett 584: 1659-1664

de Gassart A, Geminard C, Fevrier B, Raposo G, Vidal M (2003) Lipid raft-associated protein sorting in exosomes. Blood 102: 4336-4344

Dubreuil V, Marzesco A.-M, Corbeil D, Huttner WB, Wilsch-Bräuninger M (2007) Midbody and primary cilium of neural progenitors release extracellular membrane particles enriched in the stem cell marker prominin-1. J Cell Biol 176: 483-495

Eldh M, Ekström K, Valadi H, Sjöstrand M, Olsson B, Jernås M, Lötvall J (2010) Exosomes communicate protective messages during oxidative stress; possible role of exosomal shuttle RNA. PLoS One 5: e15353

Fargeas CA, Fonseca AV, Huttner WB, Corbeil D (2006) Prominin-1 (CD133): from progenitor cells to human diseases. Future Lipidol 1: 213-225

Freund D, Bauer N, Boxberger S, Feldmann S, Streller U, Ehninger G, Werner C, Bornhäuser M, Oswald J, Corbeil D (2006) Polarization of human hematopoietic progenitors during contact with multipotent mesenchymal stromal cells—effects on proliferation and clonogenicity. Stem Cells Dev 15: 815-829

Freund D, Fonseca A.-V, Janich P, Bornhäuser M, Corbeil D (2010) Differential expression of biofunctional GM1 and GM3 gangliosides within the plastic-adherent multipotent mesenchymal stromal cell population. Cytotherapy 12: 131-142

Giebel B, Beckmann J (2007) Asymmetric cell divisions of human hematopoietic stem and progenitor cells meet endosomes. Cell Cycle 6: 2201-2204

Gillette JM, Larochelle A, Dunbar CE, Lippincott-Schwartz J (2009) Intercellular transfer to signalling endosomes regulates an *ex vivo* bone marrow niche. Nat Cell Biol 11: 303-305

Huttner WB, Schiebler W, Greengard P, De Camilli P (1983) Synapsin I (protein I), a nerve terminal-specific phosphoprotein. III. Its association with synaptic vesicles studied in a highly purified synaptic vesicle preparation. J Cell Biol 96: 1374-1388

Huttner HB, Janich P, Köhrmann M, Jászai J, Siebzehnrubl F, Blümcke I, Suttorp M, Gahr M, Kuhnt D, Nimsky C, *et al* (2008) The stem cell marker prominin-1/CD133 on membrane particles in human cerebrospinal fluid offers novel approaches for studying CNS disease. Stem Cells 26: 698-705

Immervoll H, Hoem D, Sakariassen PO, Steffensen OJ, Molven A (2008) Expression of the "stem cell marker" CD133 in pancreas and pancreatic ductal adenocarcinomas. BMC Cancer 8: 48

Janowska-Wieczorek A, Majka M, Kijowski J, Baj-Krzyworzeka M, Reca R, Turner AR, Ratajczak J, Emerson SG, Kowalska MA, Ratajczak MZ (2001) Platelet-derived microparticles bind to hematopoietic stem/progenitor cells and enhance their engraftment. Blood 98: 3143-3149

Karbanová J, Missol-Kolka E, Fonseca AV, Lorra C, Janich P, Hollerová H, Jászai J, Ehrmann J, Kolár Z, Liebers C, *et al* (2008) The stem cell marker CD133 (prominin-1) is expressed in various human glandular epithelia. J Histochem Cytochem 56: 977-993

Kosodo Y, Röper K, Haubensak W, Marzesco A.-M, Corbeil D, Huttner WB (2004) Asymmetric distribution of the apical plasma membrane during neurogenic divisions of mammalian neuroepithelial cells. EMBO J 23: 2314-2324

Liu G, Yuan X, Zeng Z, Tunici P, Ng H, Abdulkadir IR, Lu L, Irvin D, Black KL, Yu JS (2006) Analysis of gene expression and chemoresistance of CD133+ cancer stem cells in glioblastoma. Mol Cancer 5: 1-12

Marzesco A.-M, Janich P, Wilsch-Bräuninger M, Dubreuil V, Langenfeld K, Corbeil D, Huttner WB (2005) Release of extracellular membrane particles carrying the stem cell marker prominin-1 (CD133) from neural progenitors and other epithelial cells. J Cell Sci 118: 2849-2858

Marzesco AM, Wilsch-Bräuninger M, Dubreuil V, Janich P, Langenfeld K, Thiele C, Huttner WB, Corbeil D (2009) Release of extracellular membrane vesicles from microvilli of epithelial cells is enhanced by depleting membrane cholesterol. FEBS Lett 583: 897-902

Méndez-Ferrer S, Michurina TV, Ferraro F, Mazloom AR, Macarthur BD, Lira SA, Scadden DT, Ma'ayan A, Enikolopov GN, Frenette PS (2010) Mesenchymal and haematopoietic stem cells form a unique bone marrow niche. Nature 466: 829-834

O'Brien CA, Pollett A, Gallinger S, Dick JE (2007) A human colon cancer cell capable of initiating tumour growth in immunodeficient mice. Nature 445: 106-110

Pike LJ (2004) Lipid rafts: heterogeneity on the high seas. Biochem J 378: 281-292

Rajendran L, Masilamani M, Solomon S, Tikkanen R, Stuermer CA, Plattner H, Illges H (2003) Asymmetric localization of flotillins/reggies in preassembled platforms confers inherent polarity to hematopoietic cells. Proc Natl Acad Sci USA 100: 8241-8246

Ratajczak J, Wysoczynski M, Hayek F, Janowska-Wieczorek A, Ratajczak MZ (2006) Membrane-derived microvesicles: important and underappreciated mediators of cell-to-cell communication. Leukemia 20: 487-495

Röper K, Corbeil D, Huttner WB (2000) Retention of prominin in microvilli reveals distinct cholesterol-based lipid micro-domains in the apical plasma membrane. Nat Cell Biol 2: 582-592

Rossi F, McNagny M, Smith G, Frampton J, Graf T (1996) Lineage commitment of transformed haematopoietic progenitors is determined by the level of PKC activity. EMBO J 15: 1894-1901

Salzer U, Prohaska R (2001) Stomatin, flotillin-1, and flotillin-2 are major integral proteins of erythrocyte lipid rafts. Blood 97: 1141-1143

Simons M, Raposo G (2009) Exosomes-vesicular carriers for intercellular communication. Curr Opin Cell Biol 21: 575-581

Simons K, Toomre D (2000) Lipid rafts and signal transduction. Nat Rev Mol Cell Biol 1: 31-39

Singh SK, Hawkins C, Clarke ID, Squire JA, Bayani J, Hide T, Henkelman RM, Cusimano MD, Dirks PB (2004) Identification of human brain tumour initiating cells. Nature 432: 396-401

Staubach S, Razawi H, Hanisch FG (2009) Proteomics of MUC1-containing lipid rafts from plasma membranes and exosomes of human breast carcinoma cells MCF-7. Proteomics 9: 2820-2835

Théry C, Boussac M, Véron P, Ricciardi-Castagnoli P, Raposo G, Garin J, Amigorena S (2001) Proteomic analysis of dendritic cell-derived exosomes: a secreted subcellular compartment distinct from apoptotic vesicles. J Immunol 166: 7309-7318

Théry C, Zitvogel L, Amigorena S (2002) Exosomes: composition, biogenesis and function. Nat Rev Immunol 2: 569-579

Théry C, Ostrowski M, Segura E (2009) Membrane vesicles as conveyors of immune responses. Nat Rev Immunol 9: 581-593

Trajkovic K, Hsu C, Chiantia S, Rajendran L, Wenzel D, Wieland F, Schwille P, Brügger B, Simons M (2008) Ceramide triggers budding of exosome vesicles into multivesicular endosomes. Science 319: 1244-1247

Vander Griend DJ, Karthaus WL, Dalrymple S, Meeker A, DeMarzo AM, Isaacs JT (2008) The role of CD133 in normal human prostate stem cells and malignant cancer-initiating cells. Cancer Res 68: 9703-9711

Weigmann A, Corbeil D, Hellwig A, Huttner WB (1997) Prominin, a novel microvilli-specific polytopic membrane protein of the apical surface of epithelial cells, is targeted to plasmalemmal protrusions of non-epithelial cells. Proc Natl Acad Sci USA 94: 12425-12430

Yin AH, Miraglia S, Zanjani ED, Almeida-Porada G, Ogawa M, Leary AG, Olweus J, Kearney J, Buck DW (1997) AC133, a novel marker for human hematopoietic stem and progenitor cells. Blood 90: 5002-5012

Zobalova R, McDermott L, Stantic M, Prokopova K, Dong LF, Neuzil J (2008) CD133-positive cells are resistant to TRAIL due to up-regulation of FLIP. Biochem Biophys Res Commun 373: 567-571

